

Location of contact residues in pharmacologically distinct drug binding sites on P-glycoprotein

¹Rituparna Mitra, ¹Megan Pavy, ²Nanditha Subramanian, ³Anthony M. George, ²Megan L. O'Mara, ⁴Ian D. Kerr & ^{1*}Richard Callaghan

¹Division of Biomedical Science & Biochemistry, Research School of Biology and Medical School, The Australian National University, Canberra, Australia

²Research School of Chemistry, The Australian National University, Canberra, Australia

³School of Life Sciences, University of Technology Sydney, Australia

⁴School of Life Sciences, University of Nottingham, Queen's Medical Centre, Nottingham, UK

Running Title:

Location of drug binding sites on P-gp

Correspondence:

*Research School of Biology, Building 134, Linnaeus Way, The Australian National University, Acton, Canberra, ACT 2601 Australia

Tel: +61 2 6125 0824

E-mail: richard.callaghan@anu.edu.au

ABSTRACT

The multidrug resistance P-glycoprotein (P-gp) is characterised by the ability to bind and/or transport an astonishing array of drugs. This poly-specificity is imparted by at least four pharmacologically distinct binding sites within the transmembrane domain. Whether or not these sites are spatially distinct has remained unclear. Biochemical and structural investigations have implicated a central cavity as the likely location for the binding sites. In the present investigation, a number of *contact residues* that are involved in drug binding were identified through biochemical assays using purified, reconstituted P-gp. Drugs were selected to represent each of the four pharmacologically distinct sites. Contact residues important in rhodamine123 binding were identified in the central cavity of P-gp. However, contact residues for the binding of vinblastine, paclitaxel and nicardipine were located at the lipid-protein interface rather than the central cavity. A key residue (F978) within the central cavity is believed to be involved in coupling drug binding to nucleotide hydrolysis. Data observed in this investigation suggest the presence of spatially distinct drug binding sites connecting through to a single translocation pore in the central cavity.

Keywords:

P-glycoprotein, multidrug resistance, membrane transport, ABC protein, cancer chemotherapy

Compounds:

Vinblastine sulphate (PubMed [CID:5388983](#)); Nicardipine hydrochloride (PubMed [CID:41114](#)); Paclitaxel (PubMed [CID:36314](#)); Rhodamine123 (PubMed [CID:9929799](#)); Adenosine triphosphate (PubMed [CID:5957](#))

1. INTRODUCTION

P-glycoprotein (P-gp) is a drug efflux pump and a member of the ATP Binding Cassette (ABC) family of proteins within the B-subfamily [1]. Its expression in cancer cells confers a drug resistant phenotype [2, 3] by preventing the accumulation of chemotherapy agents to cytotoxic levels. P-gp is capable of binding and/or transporting an astonishing number of chemically distinct compounds, whose only similarities include hydrophobicity, a planar ring system and often, the presence of a cationic nitrogen moiety [4-6]. This poly-specificity exhibited by P-gp remains an enigmatic feature that has eluded a molecular description to date.

Numerous efforts have been made to explain the complex interactions of drugs with P-gp. The standard approach was to combine drugs and ascertain whether they interacted in a competitive (one site) or non-competitive (>one site) fashion [7-10]. For example, the extent and kinetics of transport were measured for the fluorescent drugs rhodamine123 and Hoechst33342 alone, or in combination [10]. The authors demonstrated positively co-operative transport for the two probes, which indicates the presence of at least two transport-competent sites. The authors developed the nomenclature of H (Hoechst) and R (Rhodamine123) sites on the protein. Subsequent studies revealed the presence of a third (P) site that was capable of transporting prazosin [11]. In addition, these studies demonstrated that some sites are capable of binding both substrates and inhibitors.

Drug-P-gp interactions have also been investigated with photo-activate drug analogues that covalently cross-link to P-gp at their interaction site, enabling the identification of possible binding sites [12-15]. Subsequent proteolytic or chemical cleavage was used to generate peptide fragments for analysis of the regions or amino acids that had been covalently modified. Many studies observed cross-linking of the probes to both the N- and C-terminal halves of the transmembrane domain (TMD). This was initially interpreted as proof of multiple binding sites, but it is also possible that both halves of the TMD could contribute to a single site. More convincing proof of the multiple-site hypothesis was obtained in an investigation using the prazosin photoaffinity analogue [¹²⁵I]IAAP in

the presence of the modulator *cis(Z)*-flupentixol [16]. The photoaffinity probe labelled two sites on P-gp (N- and C-terminal) and the modulator only displaced labelling at the C-terminal site.

Another strategy involved the use of classical equilibrium and kinetic radioligand binding studies in order to assign competitive and allosteric interactions between drug combinations [7, 17]. This strategy enabled the demonstration of at least four pharmacologically distinct drug binding sites on P-gp. [The sites are considered “distinct” since two drugs displayed non-competitive interactions in binding assays. The spatial relationship between distinct sites is not determined by this approach.](#)

Moreover, some of these sites were shown to bind transported drugs only, one bound only modulators and another interacted with both transported substrates and modulators. Therefore, not only are there multiple sites for binding, but the outcome (i.e. transport or inhibition) for the interaction is likely dependent on the physical and chemical properties of drugs.

The consensus emerging from these different investigative approaches is that P-gp comprises a large domain to support drug interaction and that this domain may be divided into specialised binding sites for specific, chemically related compounds. According to the Jardetzky model [18], the binding sites undergo alternating access between the intra- and extra-cellular environments. Events at the nucleotide binding domains (NBDs) drive the transition of binding sites between these conformations.

A key issue to be resolved is the precise location of the drug binding domain, its constituent sites and the molecular interactions that govern binding. Structural models of mouse P-gp suggested that the central cavity of the protein was the likely region for drug binding [19, 20]. Moreover, the central cavity is lined by a number of TM helices that have been widely implicated in the interaction of drugs with P-gp during the translocation process [12, 16, 21]. This investigation proposes that individual drug binding sites lie within this central cavity and a number of amino-acid residues have been selected with the aim of identifying the locations of binding sites within the domain. Drugs that are known to bind at one of each of the four pharmacologically distinct binding

sites were used to define which residues are involved in their interaction. This systematic analysis of the mutant isoforms has identified specific “contact residues” within each of the four pharmacological sites of drug binding to P-gp.

2. MATERIALS & METHODS

2.1. Materials

The tissue culture media Insect-Xpress and Ex-Cell 405 (powder) were purchased from Lonza (Gordon, NSW) and Sigma-Aldrich (Castle Hill, NSW) respectively. Foetal Bovine Serum (heat inactivated) was obtained from Bovogen (East Keilor, Vic) and dodecyl- β -D-maltoside from Anatrace (Ohio, USA). The *E coli* total lipid extract was purchased from Avanti Polar Lipids (Alabama, USA) and the Ni-NTA His·Bind resin from Merck (Bayswater, Vic). BioBead SM-2 resin was obtained from BioRad (Gladesville, NSW) and PD-10 (8.3ml) gel permeation columns from VWR (Tingalpa, Qld) Cholesterol, imidazole, disodium adenosine triphosphate, vinblastine sulphate, nicardipine, paclitaxel, rhodamine123 and dimethyl-sulfoxide were all purchased from Sigma-Aldrich (Castle Hill, NSW). The horse-radish-peroxidase conjugated, mouse, anti-histidine monoclonal antibody was purchased from R&D Systems via BioScientific (Kirrawee, NSW). All general laboratory chemicals were of at least analytical grade and obtained from standard laboratory suppliers.

2.2. Generation of mutant P-gp isoforms and production of recombinant baculovirus

Mutations were introduced at 7 positions into a cysteine free, C-terminally His-tagged version of P-gp [22] encoded in a baculovirus expression system compatible plasmid (pFastBac_MCHS; [23]). Single cysteine isoforms M197C (TM3), A311C (TM5), F769C (TM8), F951C (TM11) and V982C (TM12) were generated in the mammalian cell expression vector pcIneo_MCHS using QuikChange mutagenesis. These isoforms were then sub-cloned into pFastBac_MCHS by BamHI/NotI mediated sub-cloning. Residues L65C (TM1) and F336C (TM6) were directly introduced into pFastBAC_MCHS using QuikChange mutagenesis. The fidelity of all mutagenesis and sub-cloning was confirmed by DNA sequencing across the entire coding sequence (SourceBiosciences, Nottingham, UK). pFastBac plasmids containing single cysteine isoforms were transformed into *E.*

coli DH10Bac competent cells and bacmid DNA isolated as previously described [24]. Bacmid DNA was verified by PCR amplification using M13 forward and reverse primers which span the integrated P-gp cDNA and all point mutations were confirmed by sequencing bacmid PCR products. Bacmid DNA was transfected into serum free Sf9 cells, and high titre viruses produced as described [24].

2.3.Expression, purification and reconstitution of P-gp mutants

P-gp was expressed in *Trichoplusia ni* (High-Five) cells following infection with recombinant baculovirus containing the specific mutant isoform. High-5 cells were purchased from Invitrogen (via Thermo-Fisher Australia) and not used beyond passage 25. Typically, $1-2 \times 10^6$ High-Five cells were treated with recombinant baculovirus at a multiplicity of infection (MOI) of 2 and the cells were grown for a period of three days post-infection. Cells were subsequently harvested by centrifugation and the pellet stored at -80°C . Crude membranes were prepared from the cells using differential ultracentrifugation following cell disruption by nitrogen cavitation as previously described [22]. Membranes were stored at -80°C at a protein concentration of $30-50\text{mg ml}^{-1}$.

P-gp was purified using immobilised metal affinity chromatography (IMAC) in a gravity based system, according to previously published methods with some modifications [22, 24]. The crude membranes (30-100mg) were suspended (5mg ml^{-1} protein) in solubilisation buffer supplemented with a 0.4% (w v^{-1}) lipid mixture (4:1 ratio of *E coli* extract:cholesterol) and 2% (w v^{-1}) dodecyl- β -D-maltoside (DDM). The DDM solubilised P-gp was mixed by slow stirring with Ni-NTA His-Bind Resin ($750\mu\text{l}$ per 100mg starting membrane) for 90 minutes at 4°C . Following binding to the resin, protein was washed sequentially with 5 bed-volumes (bv) of chromatography buffer (pH8.0) containing 20, 40 and 80mM imidazole. The chromatography buffer (pH6.8) was supplemented with 0.1% (w v^{-1}) DDM and 0.1% (w v^{-1}) lipid mixture. P-gp was eluted with

500mM imidazole and reconstituted using detergent adsorption to SM-2 BioBeads as previously described [22].

2.4.Measurement of ATP hydrolysis by mutant P-gp isoforms

ATP hydrolysis was determined by measurement of the rate of inorganic phosphate liberation by P-gp containing proteoliposomes using a modified colorimetric assay [24, 25]. In order to determine the Michaelis-Menten parameters, proteoliposomes (0.1-0.5µg protein per point) were incubated with ATP (0-1.75mM) either in the presence of 10µM nifedipine (i.e. stimulated activity) or with the solvent DMSO (i.e. basal activity). In order to investigate the potency of drugs to stimulate ATP hydrolysis, activity was measured as a function of added drug concentration (10^{-9} to 10^{-4} M) in the presence of 2 mM ATP. Following incubation (40 minutes, 37°C), the reaction was stopped by the addition of SDS and the inorganic phosphate was measured following formation of a complex with molybdate. Once the colour-forming reaction was complete, the absorbance at $\lambda=750\text{nm}$ was measured for all samples using an iMark Microplate reader. The amount of phosphate liberated was determined from extrapolation of absorbance to a standard curve of inorganic phosphate (0-20nmol P_i). In all cases the activity was expressed as µmoles of P_i liberated per minute per mg of pure protein.

The affinity for ATP (K_M) and the maximal activity (V_{MAX}) were obtained from non-linear regression of the hyperbolic relationship of activity (v) as a function of ATP concentration (S): $v = (V_{MAX} \times [S]) / (K_M + [S])$.

The potency (EC_{50}) and extent of stimulation of ATPase activity (v) were estimated by non-linear regression of the general dose-response relationship to plots of activity as a function of drug concentration ($[D]$): $v = v_{initial} + (v_{final} - v_{initial}) / (1 + 10^{(\log_{10}(EC_{50} - [D]))})$, where $v_{initial}$ is the activity in the absence of drug and v_{final} is the maximal activity observed.

2.5. Fluorescence based measurement of drug binding to P-gp

Binding of drugs to purified, reconstituted P-gp was measured through the quenching of the fluorescence of endogenous tryptophan residues [26]. Purified P-gp preparations were subjected to buffer exchange (200mM NaCl, 20mM MOPS pH6.8, 5% (v v⁻¹) glycerol, 0.1% (w v⁻¹) DDM and 0.1% (w v⁻¹) lipid mixture) to remove the imidazole used during the elution phase of chromatography. This was done prior to reconstitution using PD-10 gel permeation columns according to the manufacturer's instructions. Fractions containing purified P-gp in imidazole-free buffer were reconstituted as described earlier [24].

A minimum of 50µg protein was added to a quartz-silica fluorescence cuvette in a total volume of 1ml buffer (200mM NaCl, 20mM MOPS pH7.4). A fluorescence spectrum for the tryptophan residues was detected with $\lambda_{\text{excitation}} = 295 \pm 5 \text{nm}$ and a $\lambda_{\text{emission}}$ range from 300-500nm (emission slit width = 5nm) at a rate of 120nm min⁻¹. The range of drug concentrations (2-50µM) was achieved by sequential addition from a concentrated stock in DMSO. The solvent concentration was maintained at $\leq 1\% \text{ v v}^{-1}$, which has previously been shown not to adversely affect P-gp function [27]. Emission spectra were recorded following 5 minutes incubation post-addition of drug. Spectra were also recorded following the sequential addition of the equivalent amount of solvent to ascertain whether fluorescence was affected.

Where the addition of drug merely resulted in an alteration of the emission intensity at the λ_{max} , the intensity value was plotted as a function of drug concentration. If the drug addition resulted in alteration of λ_{max} , the extent of this wavelength shift was plotted as a function of drug concentration. In both cases, the secondary plot was hyperbolic and was fitted, by non-linear regression, with the following binding isotherm; $B = (FS_{\text{MAX}}[D]) / (K_{\text{App}} + [D])$. The change in fluorescence intensity or λ_{max} reflected the extent of drug binding, the FS_{MAX} refers to the maximal

change in fluorescence observed, K_{App} to the apparent binding affinity and $[D]$ to the drug concentration. The FS_{MAX} provides an approximation of the amount of drug bound to the protein. The K_{App} , reveals the affinity of drug interaction with the protein and an indication of the relative strength of binding.

2.6. Statistical analyses

All curve-fitting was done using non-linear least squares regression using GraphPad Prism 4 and an F-test was used for comparison of multiple curves. Comparison between multiple P-gp isoforms was performed using ANOVA with the Dunnett's post-hoc test for significance. Statistically significant differences were defined where $P < 0.05$ and all comparisons used at least three independent protein preparations.

3. RESULTS

3.1. Expression and purification of P-gp isoforms

A series of mutations was selected for investigation based on the frequency of reports implicating their involvement in P-gp function. The data involved mutagenesis [12-15], structural information [19], cysteine-directed mutagenesis [21, 28, 29] and mass spectroscopy [30]. The generation of recombinant baculovirus that produced expression of the P-gp isoforms was successful for seven single cysteine mutants and the cysteine-less (CL-P-gp) control (Figure 1). However, despite repeated attempts, expression of the F951C and F343C mutants was not achieved (data not shown).

Figure 1b shows a representative SDS-PAGE profile of fractions obtained throughout the purification procedure for CL-P-gp. Contaminating proteins were found in the flow-through fractions, which correspond to unbound material, and the 20mM imidazole wash fractions. CL-P-gp was eluted in the 500mM imidazole fraction and the band demonstrates high purity protein at a molecular weight of ~140kDa. Western immuno-blotting was used to confirm that this protein was P-gp and that following BioBead mediated reconstitution, the protein was found in lipid containing fractions. The SDS-PAGE analysis was done for each protein preparation to confirm that the level of P-gp purity was sufficient for functional assays. Typical yields for CL and the single-cysteine mutant P-gp preparations was 0.2-0.6 mg L⁻¹ insect cell culture.

3.2. Functional properties of mutant P-gp isoforms

Measurement of the basal (drug free) and drug-stimulated ATPase activity of P-gp provides a stringent assessment of the functional integrity of purified protein. ATPase activity was measured as a function of ATP concentration to generate the Michaelis-Menten parameters of affinity for nucleotide (K_M) and the maximal activity (V_{MAX}). Stimulation of ATP hydrolysis was measured in

the presence of the modulator nicardipine (10 μ M). The V_{MAX} for each mutant isoform under basal, and drug stimulated, conditions is shown in Figure 2. The cysteine-less (CL) isoform of P-gp was used as the control [for all mutant isoforms since the cysteine insertion was done into this background. Moreover, CL-P-gp isoforms](#) ~~and has~~ have previously been demonstrated to retain activity, [based on several assay systems, that was qualitatively](#) identical to the wild-type protein [22, 31, 32]. [The subtle differences from wild-type protein involve minor quantitative changes only.](#) The basal activity ($V_{MAX} = 386 \pm 36$ nmol min⁻¹ mg⁻¹) of CL-P-gp was stimulated by 3.0 ± 0.4 fold to a maximal activity of $V_{MAX} = 1048 \pm 103$ nmol min⁻¹ mg⁻¹. The affinity for ATP was similar under basal ($K_M = 0.66 \pm 0.06$ mM) and stimulated ($K_M = 0.85 \pm 0.28$ mM) conditions.

Of the 7 mutant isoforms examined only one (T769C) showed a perturbation of the basal ATPase activity, i.e. the activity in the absence of drug substrate. For T769C this manifested as a 75% reduction in basal ($V_{MAX} = 92 \pm 19$ nmol min⁻¹ mg⁻¹) compared to CL-P-gp. Despite this reduction in basal activity, T769C and all other isoforms had similar levels of nicardipine stimulated ATPase activity (682-1614 nmol min⁻¹ mg⁻¹, ANOVA $p > 0.05$) and similar degrees of stimulation (2.9-3.8 fold, ANOVA $p > 0.05$). All isoforms also retained K_M values for basal and drug-stimulated ATPase activity that were not statistically different from CL-P-gp control. Therefore, the cysteine insertion mutations used in the present investigation did not produce alterations in the protein that caused major functional perturbation. This validates their use in defining more subtle alterations in the interaction between drugs and P-gp.

Figure 3 demonstrates the assays used in the characterisation of drug interaction with the various P-gp mutant isoforms. Panel (a) provides dose-response analysis of the effects of nicardipine on ATP hydrolysis by CL-P-gp. The sigmoidal increase in ATPase activity was characterised by potency for nicardipine of $EC_{50} = 1.10 \pm 0.41$ μ M and a 2.0 ± 0.3 -fold stimulation of the activity, over the concentration range shown. The potency and degree of stimulation was assessed for all mutants with four “marker” drugs as shown in subsequent sections (tables 1-4). The four drugs nicardipine,

rhodamine123, vinblastine and paclitaxel were chosen since each of them bound to one of the four pharmacologically distinct binding sites previously described on P-gp [17].

Stimulation of ATP hydrolysis involves an initial binding of drug and then subsequent conformational changes in the TMD to enable acceleration of the catalytic process. To provide further, and more direct, assessment of the binding between drug and P-gp, the tryptophan fluorescence assay was used [26]. The assay has been widely used to characterise novel substrates/modulators of P-gp and relies on the quenching (or its relief) of fluorescence from intrinsic tryptophan residues. Hydrophobic drugs, such as those used in this study, may undergo π - π stacking interactions with tryptophan residues and thereby alter the fluorescence emission spectrum. Alternatively, the binding of drug to P-gp may alter the local environment of the tryptophan (e.g. Δ conformation or orientation) to alter its fluorescence spectrum. Figure 3(b-c) demonstrate the differential effects of nicardipine and vinblastine on the tryptophan emission spectrum of CL-P-gp. In the case of nicardipine (panel b), the maximal intensity of the emission spectrum was reduced in a dose-dependent manner. By contrast, the addition of vinblastine (panel c) caused a two-fold effect; namely a dose-dependent shift in the wavelength for maximal emission intensity (λ_{MAX}) and a corresponding increase in the intensity of the spectrum. In either case, the magnitude of the shift in response was plotted as a function of the drug concentration to generate a binding isotherm. Figure 3(d) shows the binding isotherm for vinblastine interaction with CL-P-gp obtained from five independent preparations of purified protein. The isotherm displayed a hyperbolic increase in the spectral shift of $FS_{MAX} = 33 \pm 4$ nm, which was defined by an apparent binding affinity of $K_{App} = 6.8 \pm 0.8$ μ M.

Each of the mutant P-gp isoforms was assessed for the potency of the four “marker” drugs to stimulate ATP hydrolysis as shown in Figure 3(a). Those mutations that altered the potency of drug to stimulate ATP hydrolysis were then examined for their effect on drug binding using the

tryptophan fluorescence assay as shown in Figure 3(d). In addition, at least one mutation with no alteration in ATPase activity was selected for tryptophan fluorescence analysis, to validate that changes in the potency to stimulate ATPase activity are as a result of directly altered P-gp:drug interaction. From these two functional assays, we propose that any mutation that alters the potency to stimulate ATPase activity *and* tryptophan fluorescence (K_{App}) is having a direct involvement in drug binding and is a *contact residue* for that drug. A mutation that altered ATPase activity but did not alter tryptophan fluorescence (i.e. binding to P-gp) is likely to impacts the communication between domains alter the inter-domain process involved in stimulating the rate of hydrolysis within the NBDs. Subsequent sections focus on identifying contact residues that facilitate drug binding at each of the four pharmacological sites on P-gp.

3.3. Location of residues contributing to nicardipine binding to P-gp

The dihydropyridine nicardipine is a widely used modulator of drug transport by P-gp and was shown to stimulate the basal rate of CL-P-gp by 2.0 ± 0.3 fold, with a potency of 1.1 ± 0.4 μ M (Table 1). Nicardipine also stimulated the rate of ATP hydrolysis in all seven cysteine containing mutants to an extent identical to the CL-P-gp isoform (range 1.7-3.5 fold). However, three mutant isoforms displayed a significant alteration in the potency of nicardipine to stimulate ATP hydrolysis compared to the cysteine-less control. The potencies of A311C-P-gp ($P < 0.05$) and T769C-P-gp ($P < 0.05$) were reduced approximately 3-fold by the mutation; although, as described above, the maximal extent of stimulation was unaffected. The greatest alteration in potency to stimulate ATP hydrolysis was observed for F978C-P-gp, where the EC_{50} for potency to stimulate was increased to 19.5 ± 0.4 μ M. The other isoforms did not display potencies different to the CL-P-gp, which also indicates that the introduced mutations did not significantly affect the binding of nicardipine.

In order to ascertain whether the potency alterations were due to a defect in nicardipine binding, or impaired inter-domain coupling, the tryptophan binding assay was undertaken. Nicardipine bound

to CL-P-gp with an apparent binding affinity of $K_{App} = 43.4 \pm 3.5 \mu\text{M}$ and a spectral shift of $FS_{MAX} = 44 \pm 4$ r.f.u (Table 1). The binding of nicardipine to P-gp was significantly impaired by the T769C mutation with a K_{App} value beyond the concentration of nicardipine that could be added to the assay system. Hence the K_{App} value was assigned a value of $>100\mu\text{M}$ (Table 1) and the binding capacity could also not be reliably estimated from the analysis. Amino acid 769 of P-gp was classified as a “*contact-residue*” for nicardipine and likely resides within its binding site.

The A311C and F978C mutations also caused a significant alteration in the binding of nicardipine to P-gp. Unlike the T769C mutation, they caused 2-fold increase in the affinity of nicardipine binding to P-gp (Table 1). It is possible that the amino acids at these positions directly contribute to nicardipine binding and that the mutation of the endogenous residue to cysteine improved the binding affinity. Alternatively, the mutations caused new conformational transitions of the TMDs in response to nicardipine binding that modulated tryptophan fluorescence. Subsequent sections provide further insight into the function of residue 978.

3.4. Location of residues contributing to vinblastine binding to P-gp

The anticancer drug vinblastine is a vinca alkaloid and an established substrate for transport by P-gp. Vinblastine was shown to stimulate the ATPase activity of CL-P-gp by 1.6 ± 0.1 fold, with a potency of $1.8 \pm 0.2 \mu\text{M}$ (Table 2). Vinblastine stimulated the rate of ATP hydrolysis for each of the single cysteine mutant isoforms of P-gp to a similar extent (range 1.2-3.3 fold). In addition, five of the mutations (L65C, A311C, F336C, T769C, V982C) displayed no significant difference in the potency of vinblastine to stimulate ATP hydrolysis compared to CL-P-gp. The lack of any effect on potency suggests that the binding of vinblastine to these mutants was also unaffected. To provide support for this suggestion, the binding affinity was measured for several of the isoforms. CL-P-gp bound vinblastine with a $K_{App} = 6.8 \pm 0.8 \mu\text{M}$ (Table 2), which was almost identical to the value obtained for L65C-P-gp ($K_{App} = 5.9 \pm 0.5 \mu\text{M}$). Similarly, the binding affinity measured by the

tryptophan fluorescence assay was unaffected by the F336C ($K_{App} = 11 \pm 1 \mu\text{M}$) and V982C ($K_{App} = 7.2 \pm 2.5 \mu\text{M}$) mutations. It is likely that the lack of effect of these mutations on vinblastine stimulation of ATPase activity is because the residues are not located within the vinblastine binding site.

In contrast, two of the cysteine mutations did cause marked effects on the interaction of P-gp with vinblastine. First, the M197C mutation caused a 3.7-fold reduction in potency of vinblastine to stimulate ATP hydrolysis with an $EC_{50} = 6.6 \pm 1.7 \mu\text{M}$ ($P < 0.05$), albeit with no change in the extent of stimulation (1.7 ± 0.1 fold). To ascertain whether this alteration involved a change in vinblastine binding, the effects on tryptophan fluorescence were measured. The M197C-P-gp mutant also displayed a considerable reduction in the binding affinity for vinblastine ($K_{App} = 21 \pm 5 \mu\text{M}$, $P < 0.05$), but with no effect on the maximal spectral shift. The combined effects of this mutation on the two reporter assays provide support for locating residue M197 in (or proximal to) the binding site for vinblastine.

The F978C mutation was also associated with a significant impairment in the potency of vinblastine to stimulate ATP hydrolysis, with the EC_{50} value rising 5.1-fold to $9.2 \pm 1.8 \mu\text{M}$ ($P < 0.05$) and with no change in the extent of stimulation. This mutation also affected the interaction of nicardipine with P-gp, despite the fact that it has been established that the drug binds at a pharmacologically distinct site to vinblastine [7, 17]. Notably, whilst F978C was shown to affect nicardipine binding by the tryptophan fluorescence assay, this mutation did not affect vinblastine binding since the apparent binding affinity ($K_{App} = 7.3 \pm 2.59.2 \pm 1.5 \mu\text{M}$) was identical to that of CL-Pgp. The discriminatory effects of the mutation on vinblastine interaction with P-gp indicate that residue F978 is not within the drug binding site. However, the mutation did impair the coupling between the vinblastine binding site and the NBDs, reflected in the altered vinblastine stimulation of ATPase activity.

3.5. Location of residues contributing to rhodamine123 binding to P-gp

Of the four drugs investigated, the rhodamine123 response was affected by the largest number of P-gp mutations. Rhodamine123 displayed the lowest potency to stimulate ATP hydrolysis, characterised for CL-P-gp with an $EC_{50} = 255 \pm 56 \mu\text{M}$ and a 1.8 ± 0.2 fold increase in the basal activity (Table 3). The L65C ($EC_{50} = 691 \pm 132 \mu\text{M}$) and V982C ($EC_{50} = 1181 \pm 357 \mu\text{M}$) mutations were shown to display a statistically significant reduction in the potency of rhodamine123 to stimulate ATP hydrolysis. In contrast, the F336C mutation resulted in a higher potency ($EC_{50} = 68 \pm 8 \mu\text{M}$) to stimulate ATP hydrolysis compared to the CL-P-gp isoform. The greatest effect was observed for the F978C mutant, which failed to elicit any stimulation of ATP hydrolysis by rhodamine123.

In the case of rhodamine123, the affinity for binding was increased to $>100 \mu\text{M}$, in the F978C mutant, which reflects a marked reduction in potency of binding. However, the effect on binding was not as severe as the abrogation of the ability of rhodamine123 to stimulate ATP hydrolysis. The higher K_{App} value would suggest that F978 is a *contact-residue* for rhodamine123 binding and that the dramatic effect on hydrolysis reflects a central role for this residue in conformational coupling between the binding cavity and the NBDs.

The other mutants that affected ATP hydrolysis were also associated with perturbation of rhodamine123 binding. For example, the L65C ($K_{\text{App}} = 89 \pm 25 \mu\text{M}$) and V982C ($K_{\text{App}} = 73 \pm 13 \mu\text{M}$) mutations resulted in an approximately 2-fold reduction in the potency of rhodamine123 binding to P-gp. Despite an improvement in the potency to stimulate ATP, the binding of rhodamine123 to F336C-P-gp was impaired. The K_{App} value in Table 3 was assigned a value $>100 \mu\text{M}$ since it was not possible to reach sufficiently high concentrations of rhodamine123 to generate a full hyperbola to the binding interaction. This suggests that whilst F336C is likely to be involved in rhodamine123 binding *per se*, it may also facilitate conformational changes in this binding site that couple with the NBDs.

3.6. Location of residues contributing to paclitaxel binding to P-gp

Paclitaxel stimulated ATP hydrolysis by CL-P-gp with the greatest potency ($EC_{50} = 0.55 \pm 0.09 \mu\text{M}$) of the four drugs tested (Table 4) and it increased the basal activity by 2.2 ± 0.3 fold. The degree of stimulation observed for the eight isoforms was in a tight range of 1.7 to 2.9-fold and none of the mutations altered the degree of stimulation. In addition, the L65C, M197C, F336C, T769C and V982C mutations all failed to alter the potency of paclitaxel to stimulate ATP hydrolysis, compared to the CL-P-gp isoform. Paclitaxel bound to the control CL-P-gp isoform with a dissociation constant of $K_{\text{App}} = 26 \pm 6 \mu\text{M}$. The binding of paclitaxel to P-gp was also unaffected by the L65C ($K_{\text{App}} = 21 \pm 10 \mu\text{M}$) and M197C ($K_{\text{App}} = 15 \pm 9 \mu\text{M}$) mutations, which is in agreement with their lack of effect on ATP hydrolysis.

The A311C mutation in TM5 was associated with perturbation of the interaction between paclitaxel and P-gp. This mutation caused a 5.3-fold reduction in the potency of paclitaxel to stimulate ATP hydrolysis compared to the CL-P-gp control, as demonstrated by the elevated $EC_{50} = 2.9 \pm 1.4 \mu\text{M}$ ($P < 0.05$) (Table 4). The drug binding assay also demonstrated that the A311C mutation altered the interaction of paclitaxel with P-gp. In particular, the binding dissociation constant was significantly ($P < 0.05$) reduced by 2.2-fold (compared to CL-P-gp) to $56 \pm 10 \mu\text{M}$ (Table 4). This suggests that the altered potency to stimulate ATP hydrolysis was caused by impaired binding of paclitaxel to P-gp and that residue A311 is likely to reside within the drug binding site for paclitaxel.

The F978C mutation, once again, caused altered drug interaction as shown for paclitaxel in Table 4. The potency to stimulate ATP hydrolysis was significantly ($P < 0.05$) affected, with a 7.9-fold rise in the EC_{50} value to $4.4 \pm 1.1 \mu\text{M}$, when compared to the CL-P-gp control. However, unlike the A311C-P-gp isoform, the F978C-P-gp mutation did not alter the binding affinity for paclitaxel ($K_{\text{App}} = 21 \pm 2 \mu\text{M}$), which was not significantly different to the control (Table 4). Therefore, in a situation

analogous to that observed for vinblastine, the F978C mutation did not alter binding *per se*; however, it did modulate the communication between the paclitaxel binding event and the ATP hydrolytic machinery.

4. DISCUSSION

P-gp is known to bind its vast array of substrates and inhibitors at multiple pharmacologically distinct sites [9, 10, 16, 17]. Until now the spatial location of these sites has remained elusive. In the present investigation we have identified a number of *contact residues* that are important in the binding of drugs known to interact at each of these pharmacologically distinct binding sites. This strategy has provided insight into the spatial separation of drug interaction sites on P-gp. Several mutagenesis and structural studies suggested that specific drugs bound within the central cavity of the TMD [19, 20, 28, 29, 33]. However, in the present investigation, three of the four drug binding sites had *contact residues* located at the lipid-protein interface and outside the central cavity.

The locations of the *contact residues* for each drug are shown in the molecular model of P-gp in Figure 4 and support the hypothesis of pharmacologically and spatially distinct drug binding locations within the TMD. Four *contact residues* were identified for rhodamine123 and were localised within the central cavity, proximal to its closure (or apex) near the central plane of the TMD. The interactions of the modulator nicardipine, and the transport substrates vinblastine and paclitaxel, with P-gp were only associated with a single *contact residue* each. Paclitaxel interacted closer to the extracellular region of the TMD than the rhodamine123 site. The *contact residues* for nicardipine and vinblastine were located at the protein-lipid interface of P-gp, outside of the central cavity and at a more cytoplasmic location than the rhodamine123 site.

How do our data for rhodamine123 compare with previous work on the R-site, which employed labelling of single cysteine isoforms of P-gp with a thiol-reactive rhodamine analogue and monitoring the effects on ATP hydrolysis [29]? The candidate residues identified using this approach were in broad agreement with those identified from docking and MD simulation based studies [20, 34, 35]. Another investigation using a large number of P-gp isoforms adopted a different approach using arginine enhancer mutations to identify residues within the translocation pathway [36]. However, both these investigations use a measure of overall protein activity and so

will likely identify residues that comprise the R-site for binding in addition to those in the translocation pore and involved in TMD-NBD coupling. In both studies, the residues were localised to TM helices lining the central cavity, with mutations in TM6 and TM12 featuring prominently [29, 36]. According to the murine P-gp structures many of these residues are also involved in the binding sites for two stereoisomers of a synthetic cyclic peptide [19].

The residues shown in the present investigation to mediate rhodamine123 interaction with P-gp (L65C, F336C, F978C, V982C) show some overlap with those described above. Our new data that includes direct measurement of drug binding provides strong support for the localisation of the R-site within the central cavity near its apex that forms at the cytoplasmic leaflet of the bilayer. Structural data indicates that this central cavity is accessible from the cytoplasm and the inner leaflet of the bilayer [19, 37]. The region corresponding to the R-site contains predominantly non-polar or aromatic amino acids and those identified in this study as *contact residues* for rhodamine binding are all hydrophobic.

In contrast to the data for rhodamine123, the contact residues for the other three compounds were not found within the central cavity. These residues were located at the lipid-protein interface, which concurs with the “vacuum cleaner” hypothesis of P-gp mechanism whereby transported substrates were extracted directly from the lipid milieu. This could be predicated on a drug binding site at the protein-lipid interface. Supporting evidence is provided by the highly hydrophobic probe [¹²⁵I]-INA, which could only be covalently attached to P-gp in the presence of the substrate doxorubicin [38]. [¹²⁵I]-INA is photo-activated by the chromophore doxorubicin and the cross-linking could only occur if the two compounds were in close proximity; namely, within the lipid milieu. These findings are consistent with access to substrate binding sites from the hydrophobic environment of the lipid bilayer, rather than via the cytoplasm as observed for ion transport proteins.

Location of a drug binding site proximal to the lipid-protein interface of P-gp was also provided by an elegant photoaffinity based approach [30]. P-gp was photolabelled by the substrate propafenone

and then extensively digested. The resultant fractions analysed by matrix-assisted laser desorption/ionisation time-of-flight mass spectrometry to identify those with attached propafenone. The most frequently modified residues were M197 (TM3), A311 (TM5), T769 (TM8) and F951 (TM11). Molecular modelling analysis suggested that the protein contained two binding sites that contained M197/F951 and A311/T769 respectively. The authors suggested that these proximal TM helices formed “gates” to substrate entry to a central binding site and were located at the protein-lipid interface. An alternative interpretation is that the helix pairs form distinct binding sites for drug association to P-gp, with subsequent movement of the drug through to a central translocation pore.

Three of the four residues listed in the preceding paragraph were defined in the present study as *contact residues* for drug binding to P-gp. Unfortunately, efforts to generate the F951C mutant isoform did not produce recombinant baculovirus that resulted in expression of P-gp in insect cells. However, it was shown that vinblastine interacts with M197, nicardipine with T769 and paclitaxel with A311. Although different drugs were chosen between the two investigations, there is broad agreement with respect to the amino-acids that contribute to binding sites. The TM3/11 and TM5/8 sites ~~are separated by too large a distance to form a single binding site for propafenone, which is thus assumed to interact at two sites~~ were suggested to provide individual binding sites for propafenone; in other words, propafenone can bind at two different locations on P-gp. This interpretation was based on the distance between TM3/11 and TM5/8 being too large to accommodate the binding of a single propafenone molecule to both. This is certainly not unusual since the P-gp substrate doxorubicin is also known to bind and more than one site [39]. The compounds chosen in the present investigation are more discerning in their binding sites and their characteristics of binding to P-gp indicate a single class of site for each. Vinblastine and nicardipine exhibit a complex allosteric interaction on P-gp and their binding sites are clearly distinct from a pharmacological perspective [7, 40]. Moreover, the two *contact residues* identified in the present investigation (T769 and M197) are spatially separated and a molecular model for P-gp (PDB4m1m)

predicts a separation of approximately 33Å. In addition, the two contact residues are located towards the cytoplasmic face of P-gp, within the inner hemi-leaflet of the membrane. In contrast, the contact residue for paclitaxel (A311) is located within the plane of the outer leaflet of the bilayer.

Therefore, we would propose that the central cavity of P-gp contains the R-site (and the overlapping H-site) for drug interaction with P-gp [10] and that these sites are proximal to the “apex” or “closure point” for the cavity. In addition, P-gp contains alternate drug binding sites at the lipid-protein interface, to enable extraction of drugs from the bilayer. These sites are clearly transport competent, particularly for vinblastine and paclitaxel whose efficacy is impaired by resistance conferred through P-gp expression [8]. In addition, both anticancer drugs are able to stimulate ATP hydrolysis, revealing that the binding sites are coupled to the NBDs.

Do multiple, spatially distinct, binding sites equate to multiple translocation pathways, or do they connect to a common route? Our data on the F978C mutation imply that a common route of translocation exists. Mutation of F978C resulted in impaired stimulation of ATP hydrolysis for *all* drugs tested in the present investigation, but was only a *contact residue* for rhodamine123 within the central cavity R-site. The residue has also been widely implicated to reside within the translocation pore for a number of drugs (e.g. tariquidar, verapamil, doxorubicin, morphine) [20, 36, 41]. Furthermore, residues proximal to F978 (A980), and within the central cavity (F343), have been shown by EPR-spectroscopy to undergo a shift in accessibility to a polar environment as P-gp switches between conformations in the transport process [42]. Another recent investigation has shown that F978 forms a structural motif (via hydrogen bonding to Y953) that is crucial in the propagation of ATP hydrolysis and the translocation process for several drugs that bind to P-gp with high affinity [43]. Consequently, this suggests that F978 is involved in the coupling between ATP hydrolysis in the NBDs with changes in the binding site for these three drugs.

In summary, this investigation has revealed a number of *contact residues* within the TMD of P-gp involved in binding drugs. The drugs involved were previously shown to bind at pharmacologically distinct sites on the protein, although their spatial relationship was unknown. The present investigation indicates that the site for rhodamine123 was situated within the central cavity of P-gp. In contrast, the sites for vinblastine and nicardipine were located at the interface between the TMDs and the lipid milieu. The paclitaxel binding site was located close to the central cavity, but embedded within the TMD. Therefore, this data demonstrates that the “pharmacologically distinct” sites are also spatially separated. Finally, we ~~The residues within the central cavity were associated with rhodamine123 binding and the process of coupling the TMDs to the NBDs. Contact residues for three other drugs known to interact at pharmacologically distinct binding sites are located at the lipid-protein interface.~~ We hypothesise that as P-gp switches conformational states in response to stimuli from the NBDs that the drugs are “relocated” to the central cavity that transitions into the translocation pore.

ACKNOWLEDGEMENTS

The work in this manuscript was generously supported by a project grant (#12-0008) from Worldwide Cancer Research awarded to R Callaghan, I Kerr and M O'Mara. A project grant (WT094392MA) awarded to R Callaghan and I Kerr provided partial support for the project, in particular the work of Megan Pavy.

CONFLICT OF INTEREST

The authors declare that they have no conflicts of interest with the contents of this article.

REFERENCES

- [1] M. Dean, The genetics of ATP-binding cassette transporters, *Methods Enzymol* 400 (2005) 409-29.
- [2] S.A. Carlsen, J.E. Till, V. Ling, Modulation of membrane drug permeability in Chinese hamster ovary cells, *Biochim Biophys Acta* 455(3) (1976) 900-12.
- [3] R.L. Juliano, V. Ling, A surface glycoprotein modulating drug permeability in Chinese hamster ovary cell mutants, *Biochim Biophys Acta* 455(1) (1976) 152-62.
- [4] F. Montanari, G.F. Ecker, Prediction of drug-ABC-transporter interaction - Recent advances and future challenges, *Adv Drug Deliv Rev* (2015).
- [5] T.R. Stouch, O. Gudmundsson, Progress in understanding the structure-activity relationships of P-glycoprotein, *Adv Drug Deliv Rev* 54(3) (2002) 315-28.
- [6] K. Ueda, Y. Taguchi, M. Morishima, How does P-glycoprotein recognize its substrates?, *Semin Cancer Biol* 8(3) (1997) 151-9.
- [7] D.R. Ferry, M.A. Russell, M.H. Cullen, P-glycoprotein possesses a 1,4-dihydropyridine selective drug acceptor site which is allosterically coupled to a vinca alkaloid selective binding site, *Biochem. Biophys. Res. Commun.* 188 (1992) 440-445.
- [8] C. Martin, G. Berridge, P. Mistry, C. Higgins, P. Charlton, R. Callaghan, The molecular interaction of the high affinity reversal agent XR9576 with P-glycoprotein, *Br J Pharmacol* 128(2) (1999) 403-11.
- [9] S. Orłowski, M. Garrigos, Multiple recognition of various amphiphilic molecules by the multidrug resistance P-glycoprotein: molecular mechanisms and pharmacological consequences coming from functional interactions between various drugs, *Anticancer Res* 19(4B) (1999) 3109-23.
- [10] A.B. Shapiro, V. Ling, Positively cooperative sites for drug transport by P-glycoprotein with distinct drug specificities, *Eur J Biochem* 250(1) (1997) 130-7.
- [11] A.B. Shapiro, K. Fox, P. Lam, V. Ling, Stimulation of P-glycoprotein-mediated drug transport by prazosin and progesterone. Evidence for a third drug-binding site, *Eur J Biochem* 259(3) (1999) 841-50.
- [12] E.P. Bruggemann, S.J. Currier, M.M. Gottesman, I. Pastan, Characterization of the azidopine and vinblastine binding site of P- glycoprotein, *J Biol Chem* 267(29) (1992) 21020-6.
- [13] E.P. Bruggemann, U.A. Germann, M.M. Gottesman, I. Pastan, Two different regions of P-glycoprotein [corrected] are photoaffinity- labeled by azidopine, *J Biol Chem* 264(26) (1989) 15483-8.
- [14] L.M. Greenberger, Major photoaffinity drug labeling sites for iodoaryl azidoprazosin in P-glycoprotein are within, or immediately C-terminal to, transmembrane domains 6 and 12, *J Biol Chem* 268(15) (1993) 11417-25.
- [15] L.M. Greenberger, C.-P.H. Yang, E. Gindin, S.B. Horwitz, Photoaffinity probes for the α_1 -adrenergic receptor and the calcium channel bind to a common domain in P-glycoprotein, *J Biol. Chem.* 265 (1990) 4394-4401.

- [16] S. Dey, M. Ramachandra, I. Pastan, M.M. Gottesman, S.V. Ambudkar, Evidence for two nonidentical drug-interaction sites in the human P-glycoprotein, *Proc Natl Acad Sci U S A* 94(20) (1997) 10594-9.
- [17] C. Martin, G. Berridge, C.F. Higgins, P. Mistry, P. Charlton, R. Callaghan, Communication between multiple drug binding sites on P-glycoprotein, *Molecular Pharmacol* 58 (2000) 624-632.
- [18] O. Jardetzky, Simple allosteric model for membrane pumps, *Nature* 211(5052) (1966) 969-70.
- [19] S.G. Aller, J. Yu, A. Ward, Y. Weng, S. Chittaboina, R. Zhuo, P.M. Harrell, Y.T. Trinh, Q. Zhang, I.L. Urbatsch, G. Chang, Structure of P-glycoprotein reveals a molecular basis for poly-specific drug binding, *Science* 323(5922) (2009) 1718-22.
- [20] N. Subramanian, K. Condic-Jurkic, A.E. Mark, M.L. O'Mara, Identification of Possible Binding Sites for Morphine and Nicardipine on the Multidrug Transporter P-Glycoprotein Using Umbrella Sampling Techniques, *J Chem Inf Model* 55(6) (2015) 1202-17.
- [21] T.W. Loo, D.M. Clarke, Identification of residues in the drug-binding site of human P-glycoprotein using a thiol-reactive substrate, *J Biol Chem* 272(51) (1997) 31945-8.
- [22] A.M. Taylor, J. Storm, L. Soceneantu, K.J. Linton, M. Gabriel, C. Martin, J. Woodhouse, E. Blott, C.F. Higgins, R. Callaghan, Detailed characterization of cysteine-less P-glycoprotein reveals subtle pharmacological differences in function from wild-type protein, *Br J Pharmacol* 134(8) (2001) 1609-18.
- [23] J. Storm, M. O'Mara, E. Crowley, J. Peall, P.D. Tieleman, I.D. Kerr, R. Callaghan, Residue G346 In Transmembrane Segment Six Is Involved In Inter-Domain Communication In P-Glycoprotein, *Biochemistry* 46(35) (2007) 9899-910.
- [24] E. Crowley, M.L. O'Mara, C. Reynolds, D.P. Tieleman, J. Storm, I.D. Kerr, R. Callaghan, Transmembrane helix 12 modulates progression of the ATP catalytic cycle in ABCB1, *Biochemistry* 48(26) (2009) 6249-58.
- [25] S. Chifflet, A. Torriglia, R. Chiesa, S. Tolosa, A method for the determination of inorganic phosphate in the presence of labile organic phosphate and high concentrations of protein: application to lens ATPases, *Anal Biochem* 168(1) (1988) 1-4.
- [26] R. Liu, A. Siemiarczuk, F.J. Sharom, Intrinsic fluorescence of the P-glycoprotein multidrug transporter: sensitivity of tryptophan residues to binding of drugs and nucleotides, *Biochemistry* 39(48) (2000) 14927-38.
- [27] C. Martin, G. Berridge, C.F. Higgins, R. Callaghan, The multi-drug resistance reversal agent SR33557 and modulation of vinca alkaloid binding to P-glycoprotein by an allosteric interaction, *Br J Pharmacol* 122(4) (1997) 765-71.
- [28] S. Dey, P. Hafkemeyer, I. Pastan, M.M. Gottesman, A single amino acid residue contributes to distinct mechanisms of inhibition of the human multidrug transporter by stereoisomers of the dopamine receptor antagonist flupentixol, *Biochemistry* 38(20) (1999) 6630-9.
- [29] T.W. Loo, D.M. Clarke, Location of the rhodamine-binding site in the human multidrug resistance P-glycoprotein, *J Biol Chem* 277(46) (2002) 44332-8.
- [30] K. Pleban, S. Kopp, E. Csaszar, M. Peer, T. Hrebicek, A. Rizzi, G.F. Ecker, P. Chiba, P-glycoprotein substrate binding domains are located at the transmembrane

domain/transmembrane domain interfaces: a combined photoaffinity labeling-protein homology modeling approach, *Mol Pharmacol* 67(2) (2005) 365-74.

- [31] E.J. Blott, C.F. Higgins, K.J. Linton, Cysteine-scanning mutagenesis provides no evidence for the extracellular accessibility of the nucleotide-binding domains of the multidrug resistance transporter P-glycoprotein, *EMBO J* 18 (1999) 6800-6808.
- [32] T.W. Loo, D.M. Clarke, Membrane topology of a cysteine-less mutant of human P-glycoprotein, *J Biol Chem* 270(2) (1995) 843-8.
- [33] J. Zhang, D. Li, T. Sun, L. Liang, Q. Wang, Interaction of P-glycoprotein with anti-tumor drugs: the site, gate and pathway, *Soft Matter* 11(33) (2015) 6633-41.
- [34] L. Martinez, O. Arnaud, E. Henin, H. Tao, V. Chaptal, R. Doshi, T. Andrieu, S. Dussurgey, M. Tod, A. Di Pietro, Q. Zhang, G. Chang, P. Falson, Understanding polyspecificity within the substrate-binding cavity of the human multidrug resistance P-glycoprotein, *FEBS J* 281(3) (2014) 673-82.
- [35] J.W. McCormick, P.D. Vogel, J.G. Wise, Multiple Drug Transport Pathways through Human P-Glycoprotein, *Biochemistry* 54(28) (2015) 4374-90.
- [36] T.W. Loo, M.C. Bartlett, D.M. Clarke, Identification of residues in the drug translocation pathway of the human multidrug resistance P-glycoprotein by arginine mutagenesis, *J Biol Chem* 284(36) (2009) 24074-87.
- [37] M.L. O'Mara, A.E. Mark, The Effect of Environment on the Structure of a Membrane Protein: P-Glycoprotein under Physiological Conditions, *J Chem Theory Comput* 8(10) (2012) 3964-76.
- [38] C.F. Higgins, M.M. Gottesman, Is the multidrug transporter a flippase?, *Trends Biochem Sci* 17(1) (1992) 18-21.
- [39] E.C. Spoelstra, H.V. Westerhoff, H.M. Pinedo, H. Dekker, J. Lankelma, The multidrug-resistance-reverser verapamil interferes with cellular P-glycoprotein-mediated pumping of daunorubicin as a non-competitive substrate, *Eur. J. Biochem.* 221 (1994) 363-373.
- [40] C. Martin, C.F. Higgins, R. Callaghan, The vinblastine binding site adopts high- and low-affinity conformations during a transport cycle of P-glycoprotein, *Biochemistry* 40(51) (2001) 15733-42.
- [41] T.W. Loo, M.C. Bartlett, D.M. Clarke, Suppressor mutations in the transmembrane segments of P-glycoprotein promote maturation of processing mutants and disrupt a subset of drug-binding sites, *J Biol Chem* 282(44) (2007) 32043-52.
- [42] J.H. van Wonderen, R.M. McMahon, M.L. O'Mara, C.A. McDevitt, A.J. Thomson, I.D. Kerr, F. MacMillan, R. Callaghan, The central cavity of ABCB1 undergoes alternating access during ATP hydrolysis, *FEBS J* 281(9) (2014) 2190-201.
- [43] E.E. Chufan, K. Kapoor, S.V. Ambudkar, Drug-protein hydrogen bonds govern the inhibition of the ATP hydrolysis of the multidrug transporter P-glycoprotein, *Biochem Pharmacol* 101 (2016) 40-53.

FIGURE LEGENDS

Figure 1 Expression of mutant P-gp isoforms and purification using affinity chromatography

- (a) Membranes from each of the P-gp isoforms were subjected to SDS-PAGE on 8% gels in Laemmli sample buffer. Proteins were then transferred to nitrocellulose membrane and subsequently incubated with a mouse anti-histidine monoclonal antibody conjugated with horse-radish peroxidase. Detection of P-gp was done using chemiluminescence. Equivalent sample loading (20 μ g protein) was achieved using quantitation of total protein amount. Lane assignments are as follows: (i) L65C, (ii) M197C, (iii) A311C, (iv) F336C, (v) T769C, (vi) F978C, (vii) V982C, (viii) CL and (ix) WT isoforms of P-gp
- (b) Fractions were collected at each stage of IMAC for the histidine-tagged CL-P-gp isoform and subjected to SDS-PAGE on 7% gels. Proteins were detected using PageBlue stain and an equivalent percentage (4%) of each fraction was loaded onto the gel. FT – flow through fraction of unbound protein; E₁/E₂ – elution fractions in 500mM imidazole; MW – molecular weight marker. The wash corresponds to fractions obtained in the washing steps with 20-80mM imidazole.

Figure 2 The ATPase activity of purified mutant P-gp isoforms

The Michaelis-Menten parameters for ATP hydrolysis by the CL and single cysteine containing P-gp isoforms were determined using a colorimetric assay. The histogram shows the maximal activity (V_{MAX}) for each isoform in basal (drug free; *clear bars*) and drug-stimulated (10 μ M nifedipine; *hatched bars*). The horizontal lines reveal the levels of ATP hydrolysis for the basal (*lower*) and stimulated (*upper*) activities observed for the control CL isoform. All values represent the

mean±s.e.m obtained from independent purification preparations for CL-P-gp (n=12) and the single cysteine mutants (n=4 for each).

Figure 3 ATP hydrolysis and drug binding assays for CL-P-gp

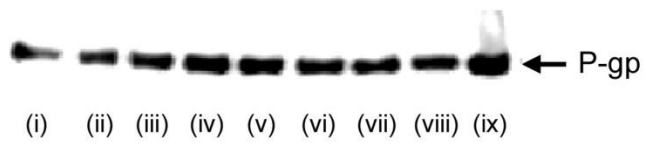
A colorimetric assay was used to determine the ATP hydrolysis activity of P-gp isoforms as described in the methods. Drug binding was assessed using the endogenous tryptophan quenching assay.

- (a) ATPase activity ($\text{nmol min}^{-1} \text{mg protein}^{-1}$) was measured as a function of nicardipine concentration. The general dose-response relationship was fitted to the data using non-linear least squares regression. Data represent the mean±s.e.m obtained from nine independent preparations of CL-P-gp.
- (b) The fluorescence emission spectra were recorded for CL-P-gp from 305-450nm in the absence (*black line*) and presence of a series of nicardipine concentrations (2-35 μM). Nicardipine was added sequentially and the solid arrow indicates the progression to increasing concentrations.
- (c) The fluorescence emission spectra were recorded for CL-P-gp from 305-450nm in the absence (*black line*) and presence of a series of vinblastine concentrations (5-35 μM). Vinblastine was added sequentially and the solid arrow indicates the progression to increasing concentrations.
- (d) The extent of the shift in λ_{MAX} for CL-P-gp in response to increasing concentrations of vinblastine was plotted as a binding isotherm. The data represent mean±s.e.m obtained from four independent preparations of P-gp. The hyperbolic binding isotherm was fitted to the data using non-linear least squares regression.

Figure 4 The distribution of *contact residues* in a homology model of P-gp

- (a) A structural model for human P-gp based on the PDB file *4m1m*, with residues mutated to cysteine in the present manuscript annotated.
- (b) The image provides a top-view of the transmembrane helices of P-gp, with other elements of the protein removed for clarity. The contact residues identified to mediate drug interactions are annotated in the image and have been depicted in red (C-terminal half) or blue (N-terminal half). The four “marker drugs” nicardipine (N), rhodamine123 (R), vinblastine (V) and paclitaxel (T) have been situated proximal to the appropriate “*contact residues*”.

(a)



(b)

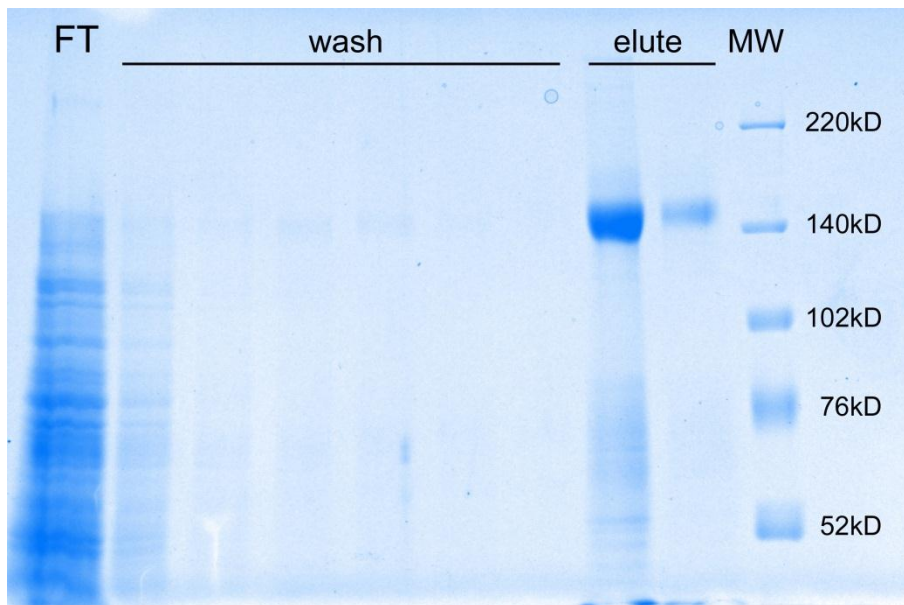


Figure 1

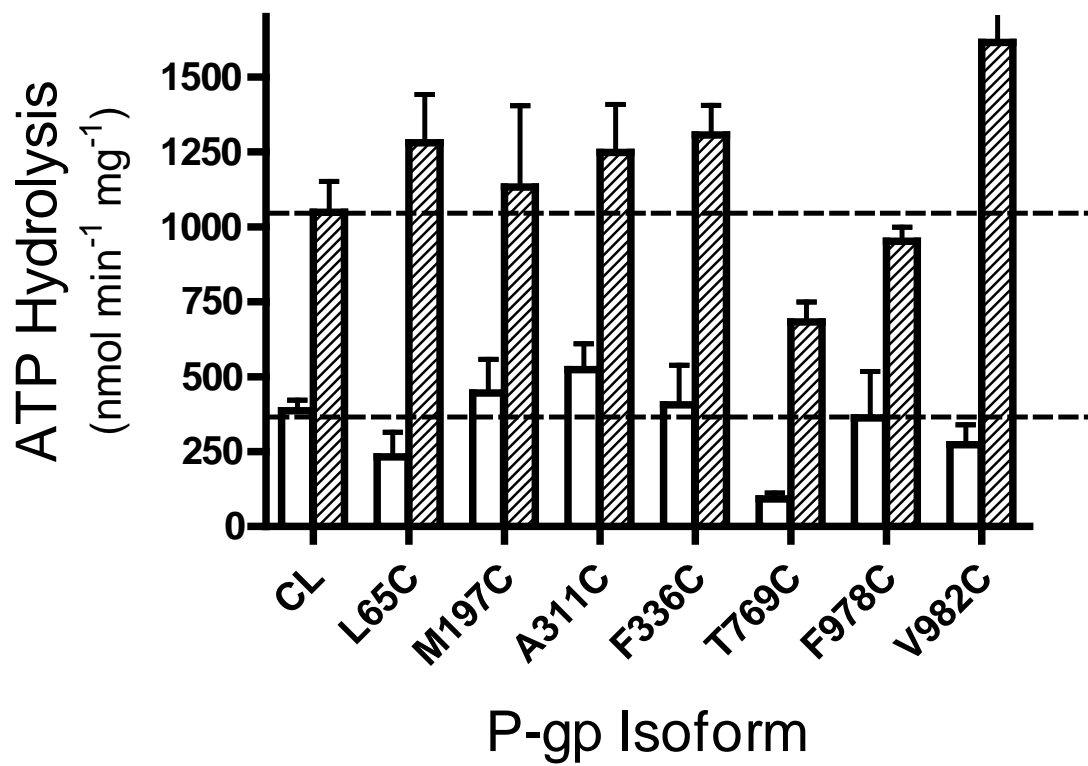


Figure 2

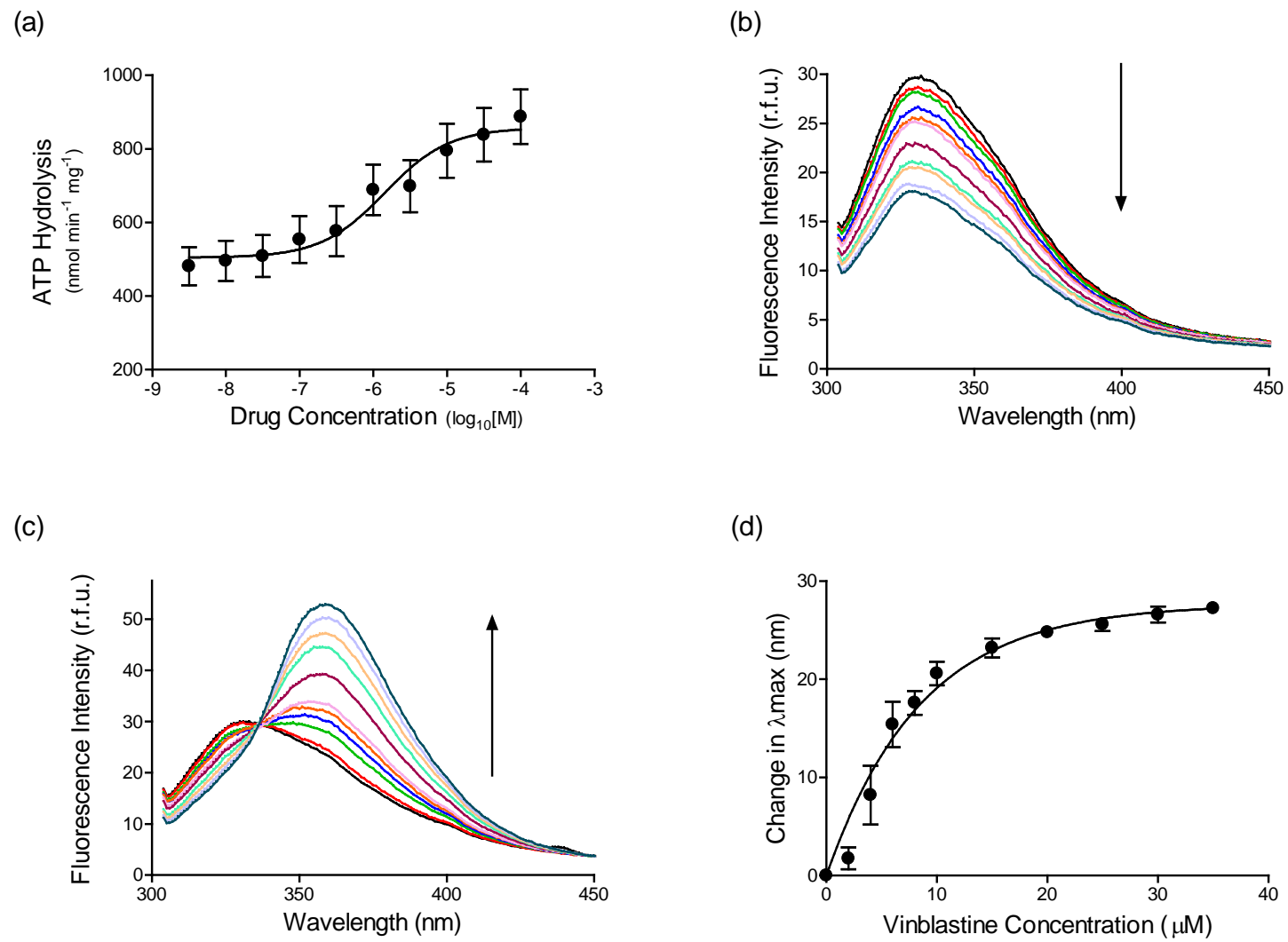
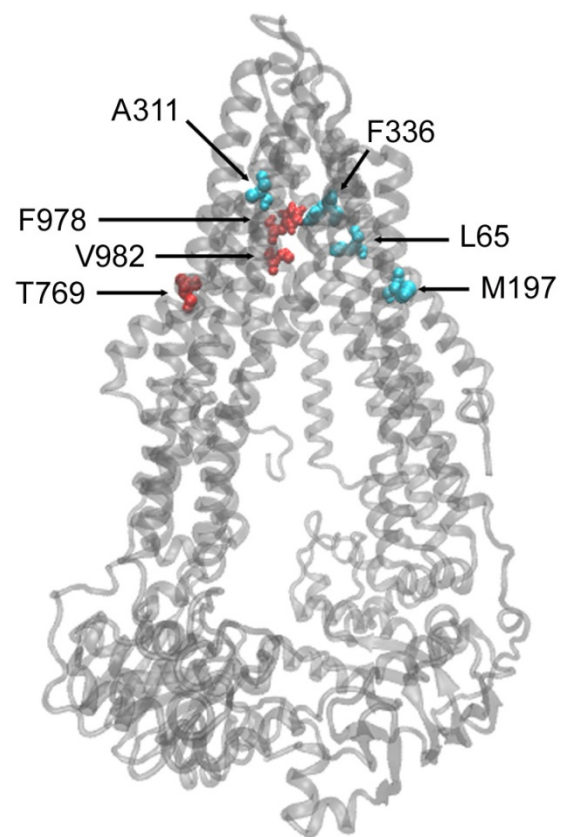


Figure 3

(a)



(b)

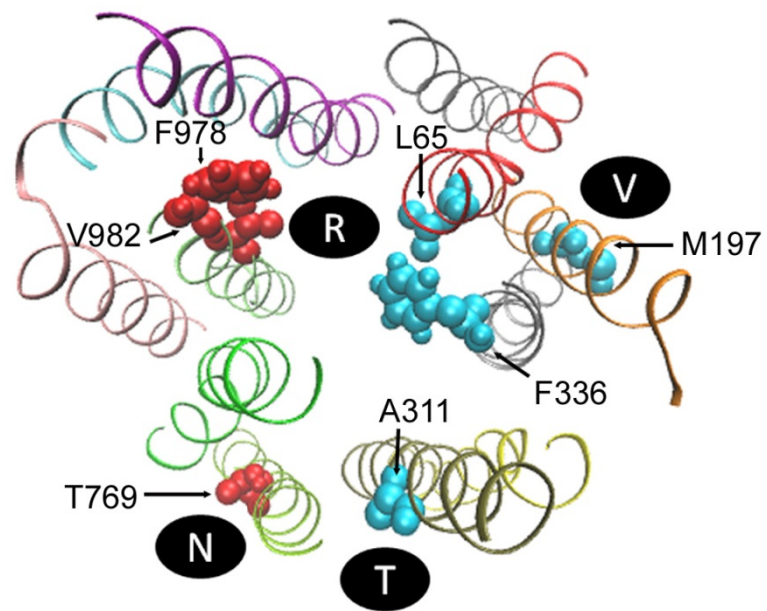


Figure 4